Accepted Manuscript

Investigation of the complex structure, comparative DNA-binding and DNA cleavage of two water-soluble mono-nuclear lanthanum(III) complexes and cytotoxic activity of chitosan-coated magnetic nanoparticles as drug delivery for the complexes

Zahra Asadi, Neda Nasrollahi, Hamidreza Karbalaei-Heidari, Vaclav Eigner, Michal Dusek, Nabiallah Mobaraki, Roya Pournejati

PII: S1386-1425(17)30048-3
DOI: doi: 10.1016/j.saa.2017.01.037
Reference: SAA 14890

To appear in: *Spectrochimica Acta Part A: Molecular and Biomolecular Spectroscopy*

Received date: 18 October 2016
Revised date: 11 January 2017
Accepted date: 18 January 2017

Please cite this article as: Zahra Asadi, Neda Nasrollahi, Hamidreza Karbalaei-Heidari, Vaclav Eigner, Michal Dusek, Nabiallah Mobaraki, Roya Pournejati , Investigation of the complex structure, comparative DNA-binding and DNA cleavage of two water-soluble mono-nuclear lanthanum(III) complexes and cytotoxic activity of chitosan-coated magnetic nanoparticles as drug delivery for the complexes. The address for the corresponding author was captured as affiliation for all authors. Please check if appropriate. Saa(2017), doi: 10.1016/j.saa.2017.01.037

This is a PDF file of an unedited manuscript that has been accepted for publication. As a service to our customers we are providing this early version of the manuscript. The manuscript will undergo copyediting, typesetting, and review of the resulting proof before it is published in its final form. Please note that during the production process errors may be discovered which could affect the content, and all legal disclaimers that apply to the journal pertain.

ACCEPTED MANUSCRIPT

Investigation of the complex structure, comparative DNA-binding and DNA cleavage of two water-soluble mono-nuclear lanthanum(III) complexes and cytotoxic activity of chitosan-coated magnetic nanoparticles as drug delivery for the complexes

Zahra Asadi[*a], Neda Nasrollahi[a], Hamidreza Karbalaei-Heidari[b], Vaclav Eigner[c], Michal Dusek[c], Nabiallah Mobaraki[a], Roya Pournejati[b]

a) Department of Chemistry, Faculty of Sciences, Shiraz University, Shiraz 71454, Iran

b) Molecular Biotechnology Laboratory, Department of Biology, Faculty of Sciences, Shiraz University, Shiraz 71454, Iran

c) Institute of Physics ASCR, v.v.i, Na Slovance 2, Praha 821182, Czech Republic

* Corresponding author. E-mail address: zasadi@shirazu.ac.ir
Tel: +98 713 6137118; Fax: +98 713 646 0788

ACCEPTED MANUSCRIPT

Abstract:

Two water-soluble mono-nuclear macrocyclic lanthanum(III) complexes of 2,6-diformyl-4-methylphenol with 1,3-diamino-2-propanol (**C_1**) or 1,3-propylenediamine (**C_2**) were synthesized and characterized by UV–Vis, FT-IR, ^{13}C and ^{1}H NMR spectroscopy and elemental analysis. **C_1** complex was structurally characterized by single-crystal X-ray diffraction, which revealed that the complex was mononuclear and ten-coordinated. The coordination sites around lanthanum(III) were occupied with a five-dentate ligand, two bidentate nitrates, and one water molecule. The interaction of complexes with DNA was studied in buffered aqueous solution at pH 7.4. UV–Vis absorption spectroscopy, emission spectroscopy, circular dichroism(CD) and viscometric measurements provided clear evidence of the intercalation mechanism of binding. The obtained intrinsic binding constants (K_b) 9.3×10^3 and 1.2×10^3 M^{-1} for **C_1** and **C_2**, respectively confirmed that **C_1** is better intercalator than **C_2**. The DNA docking studies suggested that the complexes bind with DNA in a groove binding mode with the binding affinity of **C_1** > **C_2**. Moreover, agarose gel electrophoresis study of the DNA-complex for both compounds revealed that the **C_1** intercalation cause ethidium bromide replacement in a competitive manner which confirms the suggested mechanism of binding. Finally, the anticancer experiments for the treated cancerous cell lines with both synthesized compounds show that these hydrophilic molecules need a suitable carrier to pass through the hydrophobic nature of cell membrane efficiently.

Keywords: lanthanum(III), binding constant, molecular docking, DNA cleavage, cytotoxicity, chitosan.

ACCEPTED MANUSCRIPT

ACCEPTED MANUSCRIPT

1. Introduction

The interactions of transition metal complexes with Deoxyribonucleic acid (DNA) have been studied extensively for the development of anticancer drugs [1,2]. DNA is the target molecule for many drugs especially antitumor and anticancer drugs [3-9]. Interaction of small molecules with DNA is the subject of interest in many research fields such as biochemistry, medicinal chemistry, life science, cancer therapy, etc. [10-12]. Among metal complexes, *Cisplatin* (cis-diaminodichloroplatinum(II)) is a famous and widely used anticancer drug through bonded to DNA covalently, but the usage of this drug has been limited because of its serious side effects, general toxicity, and acquired drug resistance. Thus, replacing of this drug with other suitable metal-based drugs is a necessity [4]. The serious side effect of *Cisplatin* was created from it's covalently mode of interaction. The covalent binding between the drug and DNA is irreversible and causes cell death as a result of complete inhibition of DNA processes.

Drugs with the non-covalent mode of interaction such as groove binders and intercalators are less cytotoxic than DNA-covalent agents and are reversible [13,14]. Intercalation involves π-π interactions between the planar aromatic moiety of the complex and the stacked aromatic planes of the nitrogen bases of DNA without breaking up the hydrogen bonds between the DNA bases [15-16]. An intercalator can insert between DNA base pairs deeply causing change the nucleotide structure and perturbation DNA replication and transcription. This property of intercalation agent makes them excellent candidates for the design new anticancer drugs[17].Lanthanide complexes have an ability to interact with DNA/RNA by non-covalent binding and/or cleavage the DNA/RNA chain and they are promising candidates for artificial nucleases [18-19]. In recent years a number of lanthanide complexes with intercalation mode of binding with cytotoxicity or antioxidant potentials have been reported [17,20]. Complexes of

ACCEPTED MANUSCRIPT

lanthanides with macrocyclic ligands have a desirable thermodynamic stability which is required to study their physicochemical properties in solution [21].

Nano-complexes can be used as drug-delivery agents. Among them, magnetic nanoparticles especially superparamagnetic iron oxide nanoparticles (SPIONs) play an important role in the development of drug delivery systems. Having controlled release of drugs and effective improvement of the therapeutic efficiency and minimizing the side effects of the medicine are characteristics of them. Chitosan-coated magnetic nanoparticles (CSMNPs) contain a core of magnetic material including a mixture of magnetite (Fe_3O_4) and maghemite (γ-Fe_2O_3) [22-24]. Chitosan which coated with anti-cancer drugs can be targeted to the tumor cells by an externally applied magnetic field [23,25].

In this work, we investigate two water-soluble macrocyclic Schiff base lanthanum (III) complexes prepared by (2+2) condensation of 2,6-diformyl-4-methylphenol and diamines namely 1,3-diamino-2-propanol and 1,3-propylenediamine, in the presence of the metal ion. These complexes were fully characterized by various physicochemical techniques, e.g., X-ray crystallography, elemental analyses and spectral (FT-IR, ^{13}C and $^{1}HNMR$, UV-Vis). The binding property and mode of binding of the complexes with Fish DNA under physiological conditions were studied using UV-Vis spectrophotometry, viscosity measurements, circular dichroism (CD), fluorescence spectroscopy, and molecular docking. Also, agarose gel electrophoresis technique to study the mode of binding of the complexes with plasmid DNA and MTT assay for anticancer activity measurement on MCF-7 and Jurkat cell lines were performed. As it mentioned previously, lanthanide complexes can interact by electrostatic attraction of metal(+3) ion with the phosphate backbone of DNA. On the other hand, phenylene rings and diamines were used in designing of the ligands to accelerate intercalation of aromatic rings and also caused

ACCEPTED MANUSCRIPT

hydrogen binding between N and O atoms of the ligand and DNA interior. Two different diamines were used to study the structure-activity relationship. The $\mathbf{C_1}$ complex revealed the more DNA-binding propensity than $\mathbf{C_2}$ complex. Although the gel electrophoresis study confirmed the intercalation mechanism of binding for $\mathbf{C_1}$ compound obviously but the cell viability of the cancerous cell lines in various concentrations of both compounds showed that they not pass through the cell membrane easily in their free forms and exhibit their cytotoxic effect by the help of suitable carrier like chitosan-coated magnetic nanoparticles.

2. Experimental

2.1. Analytical instruments

UV-Vis measurements were carried out on a Perkin-Elmer (Lambda 2) UV-Vis spectrophotometer equipped with a LAUDA ecoline RE 104 thermostat. The ^{1}HNMR spectra were recorded on Bruker Avance DPX 250 MHz spectrometer. ^{13}C NMR spectra were recorded using Bruker Avance DRX 500-MHz Bruker spectrometer. FT-IR spectra were recorded using Shimadzu FT-IR 8300 infrared spectrophotometer. Elemental microanalyses (C.H.N.) were obtained using a CHN Thermo-Finnigan Flash EA1112. Fluorescence spectra were carried out on a Perkin Elmer (LS 45). X-ray crystallography was performed by the four-cycle diffractometer Gemini of Agilent Technologies (Rigaku Oxford Diffraction). Circular dichroism spectra of DNA were optioned by using the Aviv Model 215 spectropolarimetre equipped with a peltier temperature control device. The BUCHI 535 instrument was used to obtain the melting point of the compounds. Viscosity measurements were carried out using the Ostwald microviscometer.

2.2. Materials

ACCEPTED MANUSCRIPT

All chemicals, except 2,6-diformyl-4-methylphenol, were used as obtained commercially, without further purification. Herring Sperm Deoxyribonucleic acid (FS-DNA), $La(NO_3)_3.6H_2O$, 1,3-diamino-2-propanol, 1,3-propylenediamine, triethyl orthoformate, absolute methanol, DMSO-d_6 for NMR spectroscopy, sodium chloride, ethylene diamine tetraacetic acid (EDTA) and Tris for buffer solution, and potassium bromide (KBr) for FT-IR spectroscopy were obtained from Merck, Fluka, Sigma and Aldrich. Agarose gel was obtained from Sangon (Shanghai) Biotechnology. Tris-HCl-NaCl buffer solution (TBS, 1 mM Tris, 5 mM NaCl, pH 7.4) was used for FS-DNA binding experiments and Tris buffer (1 mM Tris-HCl, pH 8.2, and 1 mM EDTA) for gel-electrophoresis experiments. All reagents were used as received and solvents were purified by the standard methods.

2.3. Synthesis and characterization of the complexes

2,6-diformyl-4-methylphenol was synthesized by using 4-methylphenol (Para-Cresol), paraformaldehyde, and hexamethylenetetramine according to the literature procedure [26]. Both complexes were synthesized by modifying the literature procedure [27,28]. To a vigorously stirred solution of $La(NO_3)_3.6H_2O$(1 mmol) in warm absolute methanol, triethyl orthoformate (1 mL) was added. After ten minutes a solution of 2,6-diformyl-4-methylphenol (2 mmol) was added and stirred for 10 minutes. A solution of 1,3-diamino-2-propanol (2 mmol) or 1,3-propylenediamine (2 mmol) in methanol (10 mL) was added dropwise over a period of 5 min and the reaction mixture was refluxed for 8 hours to obtain $\mathbf{C_1}$ and $\mathbf{C_2}$ complexes, respectively. Both products were obtained as a yellow precipitate, washed successively with cold methanol, and were dried in vacuum (Scheme 1).

$\mathbf{C_1}$: Yield: 57%; m.p. (>250^{o}C); F.W: 796.95; Diamagnetic; ^{1}H NMR (250 MHz, $(CD_3)_2SO$, (ppm)): 12.89(s, 2H, PhO…H…N), 8.85(s, 1H, CHOH), 8.39(s, 1H, HC=N), 8.33(s, 1H,

ACCEPTED MANUSCRIPT

HC=N), 8.14(s, 2H, HC=N), 7.41(s, 2H, Ar–H), 7.29(s, 2H, Ar–H), 6.11(s, 1H, CHOH) 4.47(s, CHOH), 4.30(s, CHOH), 4.00(d, 2H, CH_2), 3.68(br, 4H, CH_2), 3.62 (d, 2H, CH_2), 2.09(s, 6H, CH_3); ^{13}C NMR (126 MHz, $(CD_3)_2SO$, (ppm)): 171.21, 169.44 (C=N), 164.65, 146.73, 140.08, 124.94, 123.33, 115.26 (aromatic carbons), 68.94, 65.05 (CHOH), 64.00, 56.05, 54,87 (CH_2), 19.57, 19.03 (CH_3); FT-IR (KBr, cm^{-1}): 3386 $\nu_{(O–H)}$, 2932 $\nu_{(C–H)}$, 1655 $\nu_{(C=N)}$, 1442, 1384, 1292, 1230 $\nu_{(NO3)}$; Anal. Cald. for $C_{24}H_{28}N_6O_{10}La.NO_3.2H_2O$(%): C, 36.15; H, 4.04; N, 12.29; Found: C, 35.96; H, 3.98; N, 12.60; UV-Vis (Tris–HCl buffer) λ (nm) (ε ($M^{-1}cm^{-1}$)): 430(10865), 360(3520).

C_2: Yield: 55%; m.p. (>250^{o}C); F.W: 765.22; Diamagnetic; (250 MHz, $(CD_3)_2SO$, (ppm)): 12.99(s, 2H, PhO…H…N), 8.71(br, 2H, HC=N), 8.18(s, 2H, HC=N), 7.51(s, 2H Ar–H), 7.32(s, 2H, Ar–H), 4.37(t, 2H, CH_2), 3.99(br, 2H, CH_2), 3.65(br, 2H, CH_2), 3.47(br, 2H, CH_2), 2.29(m, 2H, CH_2) 2.14(s, 6H, CH_3), 1.45(m, 2H CH_2); ^{13}C NMR (126 MHz$(CD_3)_2SO$, (ppm)): 170.45, 168.00 (C=N), 165.53, 146.31, 140.01, 125.61, 123.15, 115.78 (aromatic carbons), 61.51, 51.58 36.36, 30.38 (CH_2), 19.02 (CH_3);FT-IR (KBr, cm^{-1}): 3417 $\nu_{(O–H)}$, 2916 $\nu_{(C–H)}$, 1651 $\nu_{(C=N)}$, 1442, 1381, 1319, 1227$\nu_{(NO3)}$; Anal. Cald. for $C_{24}H_{28}N_7O_{11}La.2H_2O$(%): C, 37.66; H, 4.21; N, 12.81; Found: C, 37.69; H, 4.44; N, 12.65; UV-Vis (Tris–HCl buffer) λ (nm) (ε ($M^{-1}cm^{-1}$)): 430(4555), 358(2429).

ACCEPTED MANUSCRIPT

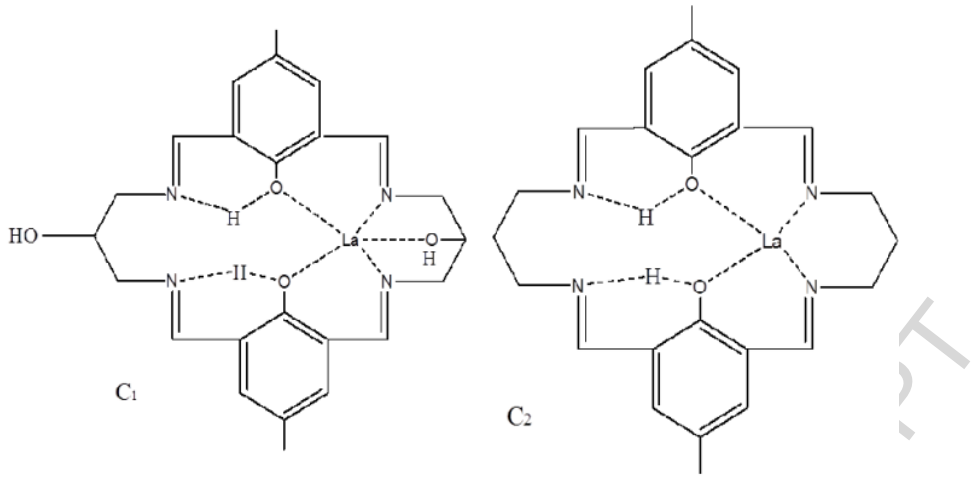

Scheme1. Structure of the complexes, nitrate groups and water are omitted for clarity.

2.4. X-ray structure analysis

Yellow crystals of **C_1** were afforded by slow evaporation of a saturated solution of the complex in a mixture of water and ethanol at room temperature. For **C_2**, attempts to prepare suitable single crystals were unsuccessful. The data were collected on Gemini diffractometer with Atlas CCD detector using graphite monochromated Mo-Kα radiation (λ = 0.7107 Å) and corrected for absorption using the CrysAlisPro software. The structure was solved by the charge-flipping method by program Superflip [29] and refined by full matrix least squares on F^2 with JANA 2006 program [30].

2.5. DNA-binding measurements

The interaction of **C_1** and **C_2** with the FS-DNA was studied by electronic absorption spectroscopy, fluorescence spectroscopy, ionic strength studies, iodide quenching studies, DNA cleavage, viscosity measurement, circular dichroism spectroscopy (CD) and molecular docking. All absorption spectrophotometric measurements were performed in thermostated quartz sample cells at 25^{o}C. DNA dissolved in buffer solution and the concentration of FS-DNA was determined from its absorption intensity at 260 nm with a molar extinction coefficient of 6600

ACCEPTED MANUSCRIPT

$M^{-1}cm^{-1}$. The ratio of UV absorbance, A_{260}/A_{280} was 1.9 that indicates the DNA was sufficiently free from protein [31]. The stock solutions of complexes ($1.0\times10^{+3}$ µM) were prepared by dissolving an appropriate amount of the complexes in 10 mL of Tris–HCl buffer. These solutions were diluted to 50µM with Tris–HCl buffer for UV-Vis spectroscopy experiments. No precipitation or turbidity was observed in solutions during a week and the UV-Vis spectral features of the complexes did not change during this time. The absorption titration was performed by insertion the increasing amount of FS-DNA to the complex solution with fixed the concentration in Tris–HCl buffer (pH = 7.4) at 25^{o}C.

Emission titration was performed with insertion the increasing amount of DNA (0 µM to $3.47\times10^{+2}$ µM) to the complex solution (0.5 µM) at 25^{o}C. The concentration of compounds was fixed and the changes in fluorescence intensity at 526 nm (excited at 430 nm) were monitored. The effect of ionic strength was studied by monitoring the changes in fluorescence intensity of the complex–DNA ([complex] = (0.5 µM), [DNA] = 40 µM) in the presence of the increasing amount of NaCl (40, 80, 160 µM). Also, the quenching effect of iodide ion (I^{-}) on the fluorescence intensity of complex-DNA was studied. The concentration of complexes (0.5 µM) and DNA (40µM) was constant and the concentration of KI increased (40, 80 µM).Viscosity measurements were carried out at constant temperature (25.0 ± 0.5^{o}C). The concentration of DNA was 100 µM, and flow time was measured with a digital stopwatch. The mean values were used to evaluate the viscosity η of the samples. The values for relative specific viscosity $(\eta/\eta_o)^{1/3}$, where η_o and η are the specific viscosity contributions of DNA in the absence (η_o) and in the presence of the complex (η), were plotted against r_i (r_i = [complex]/[DNA] = 0, 0.2, 0.4, 0.6, 0.8 and 1). Circular dichroism spectra were recorded at 25^{o}C with increasing amount of complexes (10 µ M to 80 µM) at a constant concentration of the FS-DNA (200 µM). All experiments were

ACCEPTED MANUSCRIPT

done by using 0.2 cm path cell. Each CD spectrum was collected after averaging over at least 2 accumulation using a scan speed of 100 nm min^{-1} and 1s response time.

2.6. DNA cleavage studies

DNA cleavage or interaction ability of the compounds was studied by using gel electrophoresis technique. Briefly, circular pBluescript II KS (+) plasmid DNA was incubated with different concentrations of the complexes in PBS buffer pH~7.4 for 1 hour at 37°C under both dark and UV light conditions, followed by addition of the loading buffer containing 0.25% bromophenol blue, 0.25% xylene xyanol FF and 60% glycerol (3 μL). The samples were then analyzed by 1% agarose gel electrophoresis applying Tris-acetic acid-EDTA (TAE) buffer, pH = 8.2 for 50 min, 50 V. The gel was stained with 0.5 μg/mL ethidium bromide and visualized by UV light and photographed for analysis. The cleavage or interaction efficiency was measured by determining the ability of the compounds to convert the supercoiled (SC) DNA to the nicked circular (NC) form (cleavage), or change in speed of electrophoretic movement, or lack of staining by ethidium bromide (substitution by complexes).

2.7. Cell viability assay

The cancerous cell lines were cultured in a humidified atmosphere containing 5% CO_2 at 37°C in DMEM high medium supplemented with 100 units mL^{-1} penicillin, 100 μg mL^{-1} streptomycin and 10% fetal bovine serum. Cell viability assay was performed by MTT method (Riss et al. 2013) with two cell lines, Jurkat (acute human leukemia) and MCF7 (human breast cancer). Briefly, a defined number of cells seeded in 96 well plates and incubated for 24 hours at 37^{o}C in the presence of 5% CO_2, was to the synthesized compounds in different concentrations from 10 to 250 μMin for a period of 48 hours. Afterward, 10μl MTT (3-(4,5-dimethylthiazol-2-yl)-2,5-diphenyltetrazolium bromide)solution per well was added to achieve the final

ACCEPTED MANUSCRIPT

concentration of 0.45 mg/ml and incubated for another 4 hours at 37°C. Finally, 100 µl solubilization solution (40% (vol/vol) dimethylformamide (DMF) in 2% (vol/vol) glacial acetic acid and 16 % sodium dodecyl sulfate (SDS), pH □ 4.7) was added to each well to dissolve formazan crystals and absorbance was recorded at 570 nm using Biotech ELX808 96 well reader. Cell viability percentage was calculated as follows:

Cell viability % = [A_{570} sample / A_{570} control] * 100 %

To survey the cytotoxicity effect of the complexes when were loaded on chitosan coated magnetite nanoparticles, the HepG2 hepatoma cell line was used.

C_1 and C_2 were loaded on CS-MNPs using adsorption procedure [32,33]. Briefly, 10 mg/ml and 2 mg/ml stock solution of **C_1** and **C_2** were prepared, respectively. Then 50 mg of chitosan magnetic nanoparticles dispersed in sterilized ddH_2O for 10 minutes with sonication. Finally, the compounds and CS-MNPs rotate together in 30 rpm rotation speed at 37 ˚C. The drug loading was calculated as follows:

$$\%\ Encapsulation\ capacity = \frac{Cl.Vl}{mnp} \times 100$$

Cl and Vl defined as loaded drug concentration and volume while mnp comes from the mass of nanoparticle. The cell cytotoxicity was measured with the help of MTT assay in a variety of concentration from 50 to 300 µg/ml complex-loaded CS-MNPs in a period of 48 hours.

2.8. Molecular Docking

Molecular docking studies were carried out using the Molegro Virtual Docking 6.0 (MVD) software [34]. This software generates the best DNA-ligand configurations according to several scoring criteria such as Moldock and Rerank scores. In MVD the units are arbitrary, In MVD the units are arbitrary, but an ideal hydrogen bond contributes to the overall energy [35]. The crystal

ACCEPTED MANUSCRIPT

structure of DNA, PDB code: 4HC9 d(TTTTTGGCCCCCAAAAAAAA) was taken from the protein Data bank (www.rsbs.org/pdb) [36], all other molecules in this structure were removed before performing docking calculations. Then, the X-ray structures of **C_1**, **C_2** [37] and DNA were imported to Molegro Virtual Docker (MVD) [37] to carry out the docking calculations. The binding site was chosen by (x=8, y=-107, z=50, and radius=28), which covered all the DNA strand base pairs. We have selected score as Moldock score [GRID], with GRID resolution of 0.3 Å. Algorithm selected for docking was Moldock along with a number of runs as 20 for each docking calculation, 10 different poses were requested. All other parameters were kept at their default values. Parameter settings pose generation and simplex were evolution selected as default settings.

3. Results and discussion

The complexes were prepared by (2+2) condensation of 2,6-diformyl-*p*-cresol and 1,3-diamino-2-hydroxypropane or 1,3-diaminopropane in the presence of $La(NO_3)_3.6H_2O$. The complexes were stable in air, soluble in water and dimethylsulfoxide (DMSO), slightly soluble in acetone, ethanol, and methanol. **C_2** complex was also slightly soluble in ethyl acetate and chloroform. The elemental analysis proposed $C_{24}H_{28}N_6O_{10}La.NO_3.2H_2O$ formula for **C_1**, while $C_{24}H_{28}N_6O_{10}La.NO_3.H_2O.1.51(O)$ formula was confirmed by single crystal X-ray crystallography (here 1.51(O) stands for the disordered lattice water where hydrogen atoms could not be determined).

The FT-IR spectra of the complexes were recorded in the region 4000–400 cm^{-1}. Both **C_1** and **C_2** complexes were characterized by a strong band due to $\nu_{(C=N)}$ at 1655 and 1651 cm^{-1}, respectively. The absorption bands of the coordinated nitrates were observed at about 1442,

ACCEPTED MANUSCRIPT

1384, 1292, 1230 cm^{-1} for $\mathbf{C_1}$ and 1442, 1381, 1319, 1227 cm^{-1} for $\mathbf{C_2}$ suggesting bidentate coordination of nitrate groups to La(III) center [38].

Electronic spectral data of the complexes in water are given in the experimental part. By considering the electronic spectra of the complexes with the electronic spectrum of 2, 6-diformyl-4-methylphenol, the bands around 250 and 360 nm of two complexes were attributed to intramolecular π-π* transition in aromatic rings or imines groups and the other bands at 430 nm were attributed to n-π* phenol groups (Fig. 1) [38].

The ^{13}C NMR spectra of both complexes indicated the asymmetric structure of the macrocyclic of the metal ion in one of the two its compartments. For both complexes two different the azomethine carbon resonance was observed at 168.0 - 171.21 ppm. In the ^{13}C NMR spectra of $\mathbf{C_1}$, aliphatic alcoholic carbons were observed at 68.94 and 65.05 ppm. In the $^{1}HNMR$ spectrum of $\mathbf{C_1}$, the signal of phenolic hydrogen was observed at 12.89 ppm (PhO$^{\cdots}$H$^{\cdots}$N). Because the aliphatic alcoholic groups were not deprotonated, the signal at 8.85 ppm was assigned to the coordinated alcoholic group while the one at 6.11ppm was assigned to the uncoordinated one. Two different imine signals were observed at 8.39 and 8.33 ppm due to the asymmetric structure of the macrocyclic complex. The signals assigned to the phenolic hydrogen of $\mathbf{C_2}$ were at 12.99 ppm and of the imine hydrogens at 8.71 and 8.18 ppm.

ACCEPTED MANUSCRIPT

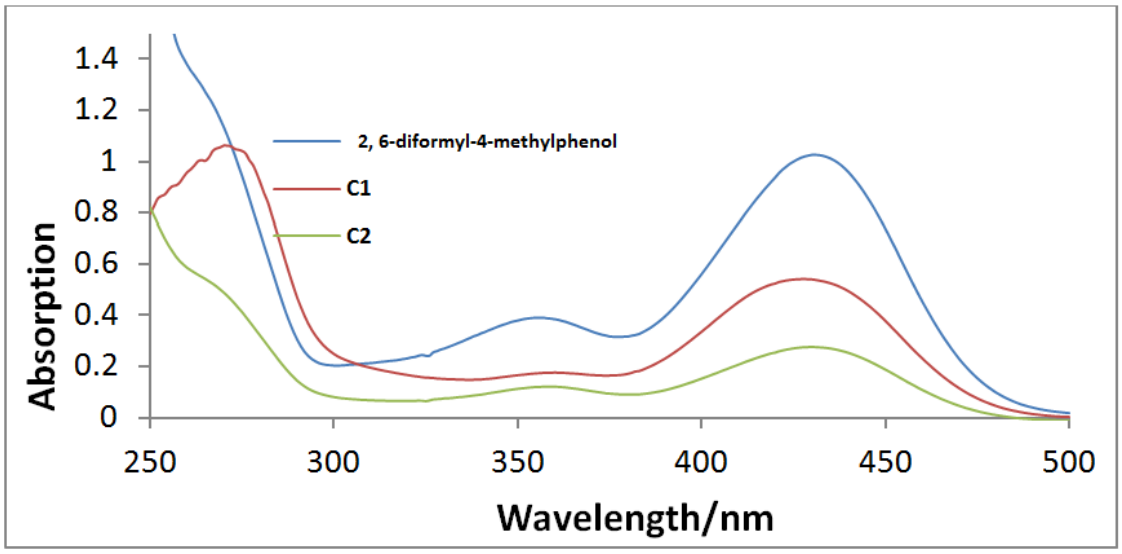

Figure1. A comparison of the electronic spectrum of the 2, 6-diformyl-4-methylphenol, $\mathbf{C_1}$ and $\mathbf{C_2}$ complexes(50μM) in Tris–HCl buffer at room temperature.

3.1. Structure description

The single crystal X-ray structure analysis revealed that $\mathbf{C_1}$ crystallized in a monoclinic crystal system with space group *C*2/*c*. The asymmetric unit (Fig. 2) consisted of one mononuclear La(III) complex ($C_{24}H_{28}N_6O_{10}La$), two bidentate coordinated nitrate groups and one coordinated water molecule as a solvent of crystallization. Moreover, the structure contained one free nitrate, counter ion and approximately 1.5 molecules of disordered lattice water. The disorder prevented determination of hydrogen atoms for lattice water; instead, we refined occupancy of oxygen atoms in order to describe also the electron density corresponding to the missing hydrogen atoms.

The metal center was ten-coordinated with two nitrogen atoms and three oxygen atoms of the macrocycle ligand, four oxygen atoms of the two chelating nitrate groups, and an oxygen atom of the coordinated water. The macrocycle ring was folded, taking a V shape. The La-O2, La-O3 and La-O4 bond lengths were found to be 2.419(1)Å, 2.544(2)Å and 2.439(1)Å respectively,

ACCEPTED MANUSCRIPT

which suggested that the La-O (phenolic) bonds were stronger than the La-O(H) bond. The La-N2 and La-N3 bond lengths 2.673(2)Å and 2.704(2)Å that the La-O bonds were stronger than La-N(imine) bonds. The bond lengths of the coordinated nitrate groups La-O2n, La-O3n, La-O4n, and La-O5n were found to be 2.790(1)Å, 2.632(2)Å, 2.779(2)Å and 2.689(2)Å, respectively, suggested that the ligand bonds were stronger than nitrate bonds. The bond length of the La-O1w (2.527(1)Å) was in the range of the La-O(macrocycle) bond lengths. Difference Fourier maps revealed that the hydrogen atoms of the imine groups (N1, N4) are present, and they were refined using the distance restraint 0.86 Å. These hydrogens atoms, H1n1 and H1n4, participated in strong hydrogen bonds to the oxygen atoms of the aromatic rings (O2, O4), and also in slightly weaker hydrogen bonds to the oxygen atom O5n belonging to one of the coordinated nitrate groups. Other coordinating atoms of the macrocycle ligand O3, also kept its hydrogen atom, as well as the non-coordinated O1. Thus interesting feature of this structure is that deprotonation occurred.

The crystal data and parameters are listed in Table 1. Selected bond lengths and angles are summarized in Table 2.

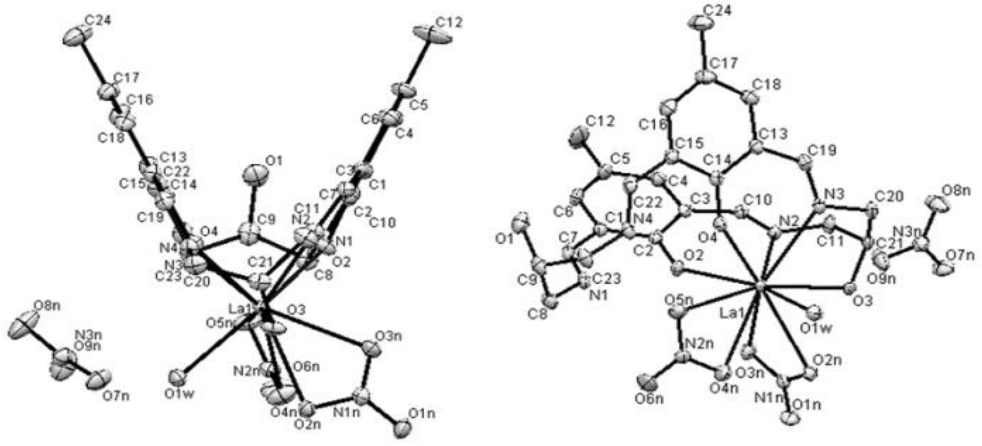

Figure2. ORTEP representation of $\mathbf{C_1}$, the hydrogen atoms have been omitted for clarity

ACCEPTED MANUSCRIPT

Table 1. Crystal data and structure refinement for C_1

	Complex
Formula	$C_{24}H_{30}LaN_6O_{11.}NO_3.1.51(O)$
Temperature/K	120
Crystal system	monoclinic
Space group	*C2/c*
a [Å]	23.4065(12)
b [Å]	16.3131(8)
c [Å]	17.5394(11)
α [˚]	90
β [˚]	111.865(5)
γ [˚]	90
vol/Å^3	6215.4(6)
Z,*Z*′	8
D, g/cm^3	1.717
μ [mm^{-1}]	1.46
F(000)	3232.8
$R[F^2>3\sigma(F^2)]$=0.024R(reflections)	
$wR(F^2)$=0.073	

ACCEPTED MANUSCRIPT

ACCEPTED MANUSCRIPT

Table 2. Selected bond lengths (Å) and angles (°) for $\mathbf{C_1}$

Bond angles (°)		Bond lengths (Å)	
O2 La O4	74.68(5)	La-O2	2.419(1)
O2 La O1w	151.87(5)	La-O3	2.544(2)
O2 La O2n	119.41(5)	La-O	2.439(1)
O2 La O3n	74.07(5)	La-O1	2.527(1)
O2 La O4n	91.56(5)	La-O2n	2.790(1)
O2 La O5n	67.33(5)	La-O3n	2.632(2)
O2 La N2	68.99(5)	La-O4n	2.779(2)
O2 La N3	110.84(5)	La- O5n	2.689(2)
O3 La O4	130.58(5)	La-N2	2.673(2)
O3 La O1w	82.27(5)	La -N3	2.704(2)
O3 La O2n	59.12(4)		
O3 La O3n	76.29(5)		
O3 La O4n	116.31(5)		
O3 La O5n	161.13(5)		
O3 La N2	61.36(5)		
O3 La N3	64.58(5)		
O4 La O1w	89.91(5)		
O4 La O2n	156.38(4)		
O4 La O3n	147.57(5)		
O4 La O4n	106.12(5)		
O4 La N2	97.41(5)		
O4 La N3	66.04(5)		
O1w La O3n	114.45(5)		
O1w La O4n	69.92(5)		
O1w LaO5n	84.76(5)		
O1w LaN2	137.55(5)		
O1w La N3	82.77(5)		
O2n La O3n	46.75(4)		
O2n LaO4n	57.58(5)		
O2n La O5n	103.32(5)		

3.2. Electronic absorption titration

Electronic absorption spectroscopy was used to examine the binding mode and binding affinity of metal complexes with DNA [39]. In this regard, by monitoring the change in absorption intensity, the equilibrium binding constant (K_b) and the binding site size (s) of the complex to DNA was calculated. Spectrophotometric titration of $\mathbf{C_1}$ and $\mathbf{C_2}$ with FS-DNA in

ACCEPTED MANUSCRIPT

Tris-HCl buffer is shown in Fig. 3. With increasing in molar ratio (r) of FS-DNA to complexes (r = 0-10), an isosbestic point about 375 nm, and the ligand-centered n→π* absorption bands (about 430 nm) showed a decrease in molar absorptivity (hypochromism 80%, 20% for **C_1** & **C_2**, respectively). A significant red shift in the absorbance maxima for **C_1** (9 nm), and for **C_2** (1 nm) was observed. Besides, hyperchromism of the band around 350nm with a slight blue shift was observed for both complexes. The overall spectral changes with isosbestic point suggested a strong interaction. Hypochromism and bathochromism of the absorption intensity indicated that the mode of binding to DNA was intercalation, involving partial insertion of the aromatic chromophore in between the base pairs of DNA [40]. Typical intercalators, caused red shift >15 nm, and the hypochromism >35% [41]. By decreasing the distance between the intercalated complex and DNA bases, after binding, hypochromism was observed because of the strong π→π* stacking interaction between aromatic chromophore of the macrocycle ligand and the base pair of DNA. The extent of the hypochromism is consistent with the strength of the intercalative interaction [42]. Red-shift (bathochromism) was also observed as a result of decreasing the energy level of π→π* electron transition after binding of the complex to DNA. As DNA is a polyanion, the pre-association step is particularly significant if the metal complex is cationic in nature [43]. The electrostatic attraction between the positive charge of the La(III) complexes and the backbone phosphate groups stabilized the complex-DNA interaction, and at the following step favor intercalation. The positive charge causes a lowering in the LUMO energy of the complex, favoring the interaction with HOMO of the DNA bases [13]. Other electrostatic effects such as hydrogen bonding between the complexes and the base pairs of DNA may occur. Because of electrostatic attraction between the complexes and DNA, hyperchromism with a slight blue shift was observed around 350 nm for both complexes. Hyperchromism may be

ACCEPTED MANUSCRIPT

indicative of groove binding which reflects the changes of conformation and structure of DNA after the interaction occurred [13].The strength of binding is directly related to the extent of decreasing or increasing in absorption intensity and the amount of bathochromism or hypsochromism. By considering Fig.3, it was concluded that the interaction of **C_1** with DNA is stronger than **C_2**.

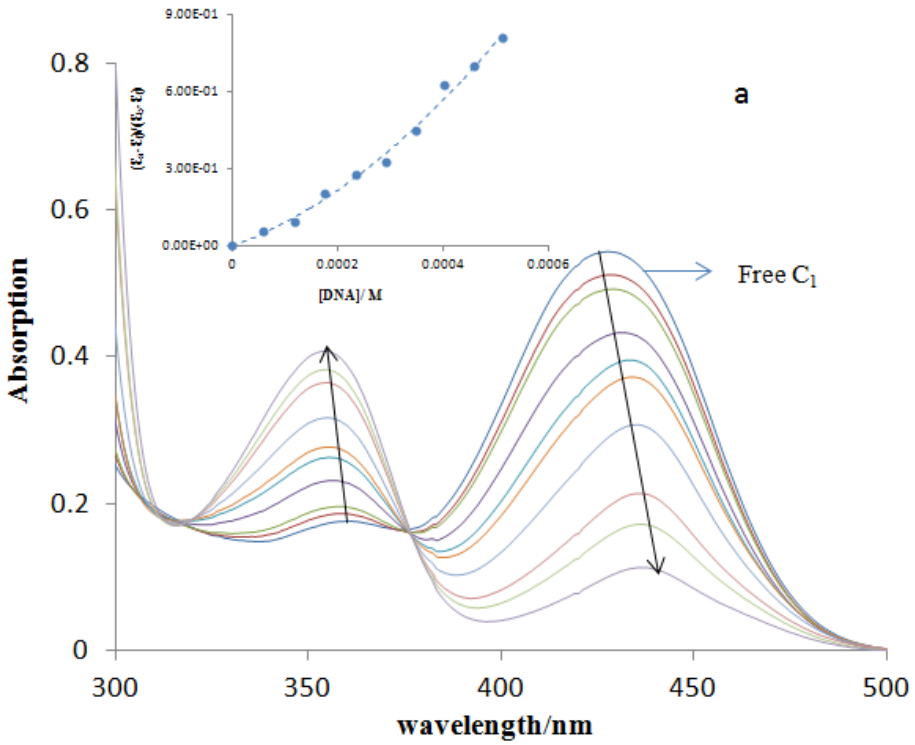

ACCEPTED MANUSCRIPT

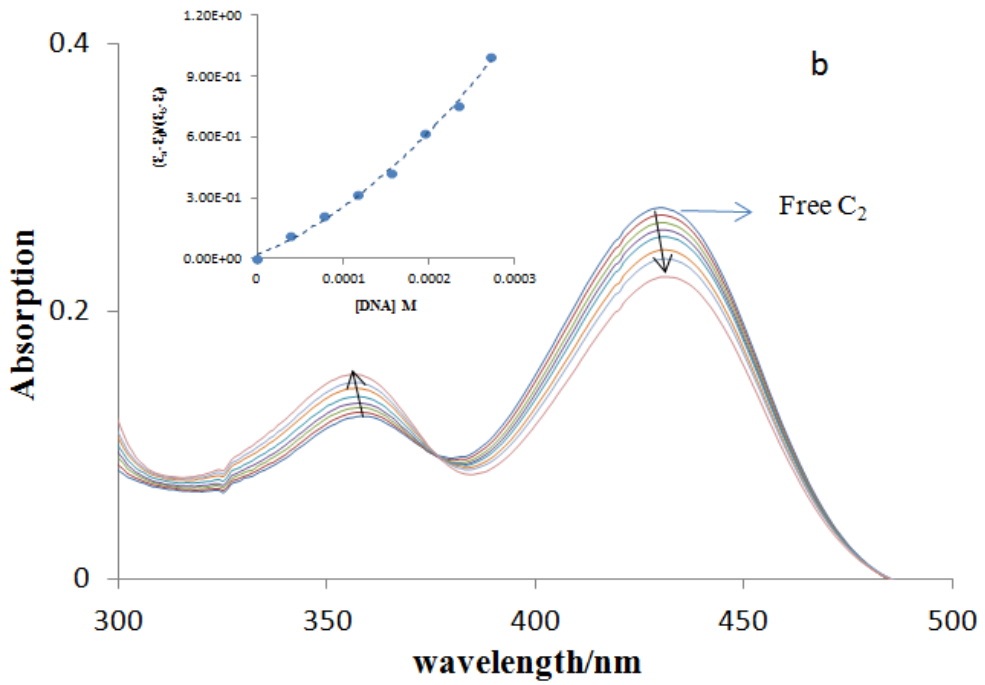

Figure3. Spectrophotometric titration $\mathbf{C_1}$ (a) and $\mathbf{C_2}$ (b) complexes with DNA(0-512 µM) in Tris–HCl buffer as the DNA/complexes molar ratios varying from 0 to 10 at 25^0C. The inset shows Plot of $(\varepsilon_a-\varepsilon_f)/(\varepsilon_b-\varepsilon_f)$ versus [DNA] for the $\mathbf{C_1}$(a) and $\mathbf{C_2}$(b) complexes.

In order to investigate quantitatively the binding strength, the intrinsic binding constant, K_b, and the stoichiometry (s) were determined by using equation (1a ,1b) [44,45]:

$$(\varepsilon_{a-}\varepsilon_f)/(\varepsilon_{b-}\varepsilon_f) = \left(b - \sqrt{(b^2 - 2K_b{}^2\, C_t[DNA]/s)}\right)/2K_b\, C_t \qquad (1a)$$

$$b = 1 + K_b\, C_t + K_b[DNA]\,/\,2s \qquad (1b)$$

Where ε_a, ε_b, and ε_f are apparent absorption coefficient, ε_a is the extinction coefficient observed for the absorption band at a given DNA concentration, ε_f is the extinction coefficient of the complexes in its free form and ε_b of the complex in the fully bound form. C_t is the total concentration of the metal complexes and s is the binding site size. A plot of $(\varepsilon_a-\varepsilon_f)/(\varepsilon_b-\varepsilon_f)$ versus [DNA] are shown in Fig. 3.

ACCEPTED MANUSCRIPT

The intrinsic binding constant, K_b, of $\mathbf{C_1}$ and $\mathbf{C_2}$ complexes, was obtained 9.3×10^3 and 1.2×10^3 M^{-1}, respectively, which is consistent with the observed trend in hypochromism, and *s* values for both complexes were 1.1. The values of K_b were comparable to that observed for some intercalator complexes like Bu_3SnL (6.05×10^3 M^{-1}), Cy_3SnL (2.30×10^3 M^{-1}), Ph_3SnL (3.25×10^3 M^{-1}), L = 4-(4-nitrophenyl)piperazine-1-carbodithioate [46], $[Cu(LMF)(Gly)(H_2O)_2]$ $Cl.2H_2O$ (7.98×10^3 M^{-1}), $[Ni(LMF)(Gly)(H_2O)_2]Cl.H_2O$ (3.57×10^3 M^{-1}), $[Co(LMF)(Gly)(H_2O)_2]$ .Cl (2.43×10^3 M^{-1}), and $[Zn(LMF)(Gly)(H_2O)_2].Cl$($1.47\times10^3$ M^{-1}) [47]. The binding affinity (K_b) for $\mathbf{C_1}$ and $\mathbf{C_2}$ was smaller than for the classical intercalator ethidium bromide (K_b = 1.4×10^6 M^{-1}) [48]. K_b values clearly revealed that binding affinity of $\mathbf{C_1}$ is larger than the one for $\mathbf{C_2}$, and such result may be attributed to the presence of the alcoholic groups and La-O bond in $\mathbf{C_1}$ structure**.** The former causes extra hydrogen bonding between the complex and DNA interior and the latter decrease the electron density on the metal and caused a better Lewis acidity character of lanthanum(III) toward DNA bases. Additionally, by comparing the structure of complexes, it is clear that the macrocycle ring of $\mathbf{C_1}$ was more folded than $\mathbf{C_2}$ [37], thus $\mathbf{C_1}$ intercalated into the base stacks of DNA more deeply than $\mathbf{C_2}$ and was a better intercalator.

3.3. Fluorescence spectral studies

For confirming the binding mode of the interaction, emission experiments were carried out [49]. Two complexes exhibited strong emission bands with a maximum at 526 nm (excited at 430 nm). For both complexes enhancement in intensity was observed with increasing FS-DNA concentration (Fig. 4) and this enhancement was larger for $\mathbf{C_1}$ confirming more effective interaction with DNA [13]. The extent of enhancement in intensity is directly related to the extent to which the complexes penetrated into the hydrophobic media inside the DNA [50]. The enhancement avoided the quenching effect of the solvent water molecule, thus the enhancement

ACCEPTED MANUSCRIPT

of the intensity confirmed the intercalation mode of binding of these complexes in agreement with absorption studies [51]. Fluorescence data were analyzed according to the Stern–Volmer equation (2):

$$\frac{F_0}{F} = 1 + K_{SV}\,[E] = 1 + K_e\,\tau_0\,[E] \qquad (2)$$

Where F and F_0 are the fluorescence intensities in the presence and the absence of the enhancer, respectively. K_{SV} is the Stern−Volmer enhancing constant, [E] is the concentration of the enhancer, K_e is the bimolecular enhancing constant and τ_0 is the average lifetime of the biomolecule in the absence of the enhancer, and its value is 10^{-8}s [52,53]. The obtained Stern−Volmer plots for both **C_1** and **C_2** were nonlinear (Fig. 5). These results represent the existence of two modes of interaction, static and dynamic, between the complexes and DNA [54,55]. Calculation of the Stern−Volmer constant (K_{SV}) and the enhancing rate constant (K_e) were not possible for the nonlinear Stern−Volmer plots, thus Lineweaver-Burk (LWB) equation (3) was used [55].

$$1/(F_0 - F) = 1/F_0 K_b\,[Q] + 1/F_0 \qquad (3)$$

Where, F_0 and F are the fluorescence intensities in the absence and presence of the quencher at the concentration $[Q]$. In the case of **C_1** and **C_2**, the emission intensity was enhanced, thus the equation becomes equation (4):

$$1/(F - F_0) = 1/F_0 K_b\,[E] + 1/F_0 \qquad (4)$$

[E] is the concentration of the enhancer. The binding constants (K_b) were calculated from the ratio of intercept to the slope. The K_b values for **C_1** and **C_2** complexes were $3.64\times10^4 M^{-1}$ and

ACCEPTED MANUSCRIPT

$5.15\times10^{3}M^{-1}$ respectively (Fig. 6). These results confirmed that the interaction of **C_1** with FS-DNA was stronger than that of **C_2**.

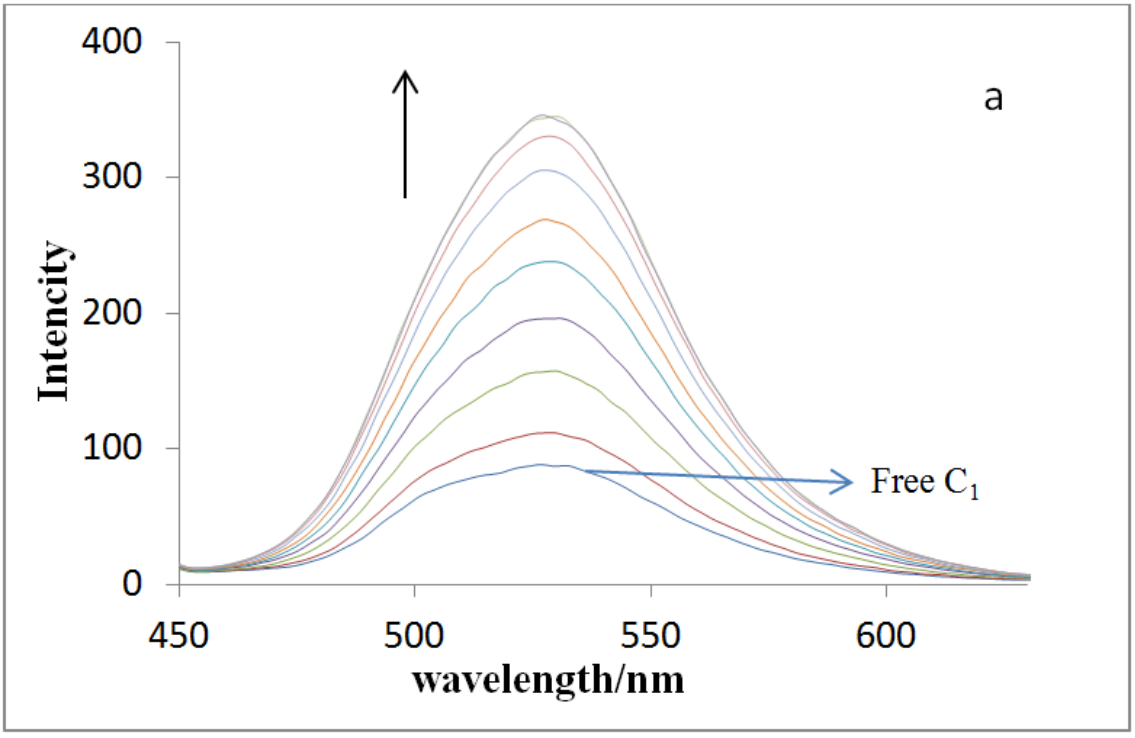

ACCEP

ACCEPTED MANUSCRIPT

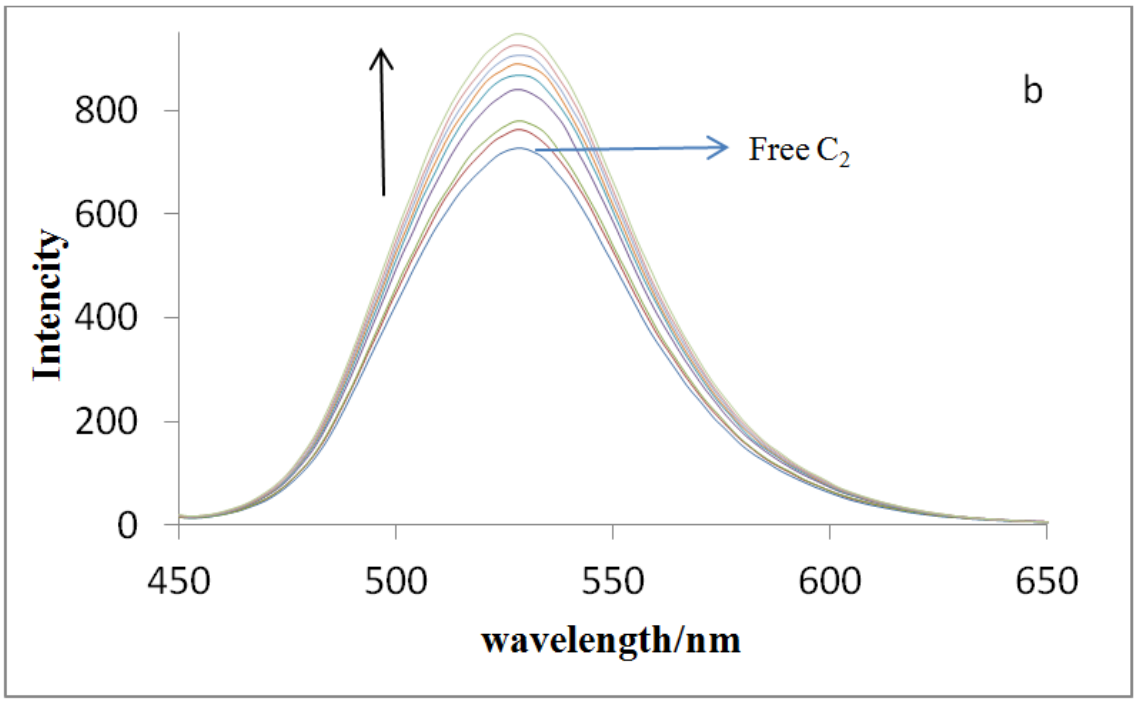

Figure4. Fluorescence titration of (a) $\mathbf{C_1}$ and (b) $\mathbf{C_2}$, at 526 nm, with DNA(0 µM to 347 µM) in Tris–HCl buffer at room temperature

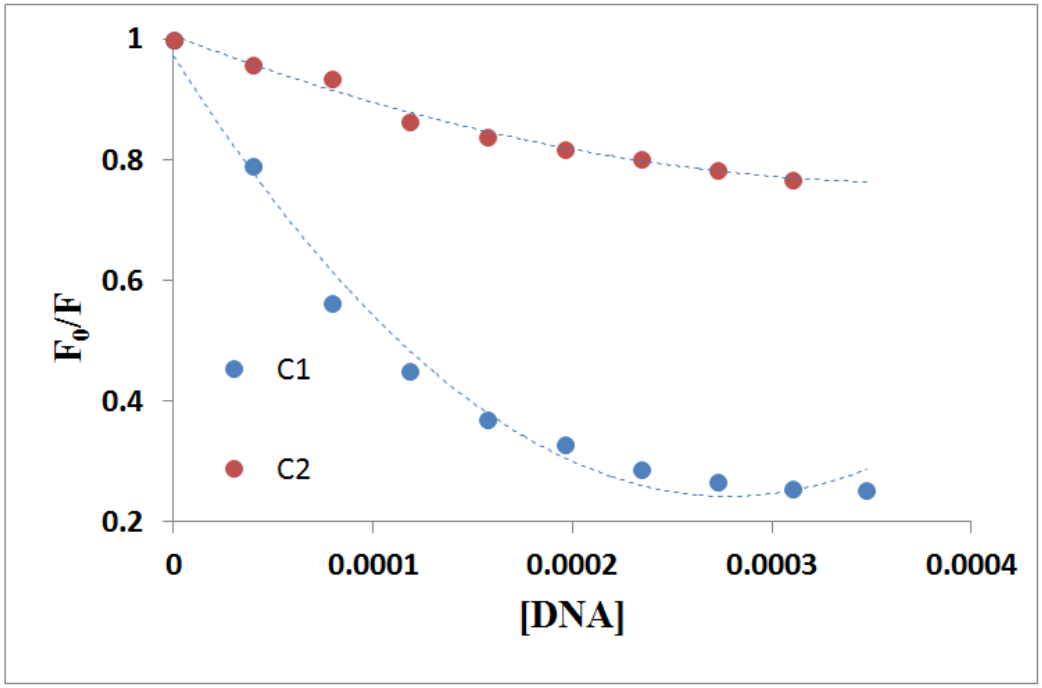

Figure5. The Stern–Volmer plots for $\mathbf{C_1}$ and $\mathbf{C_2}$ complexes, at 526 nm at room temperature

ACCEPTED MANUSCRIPT

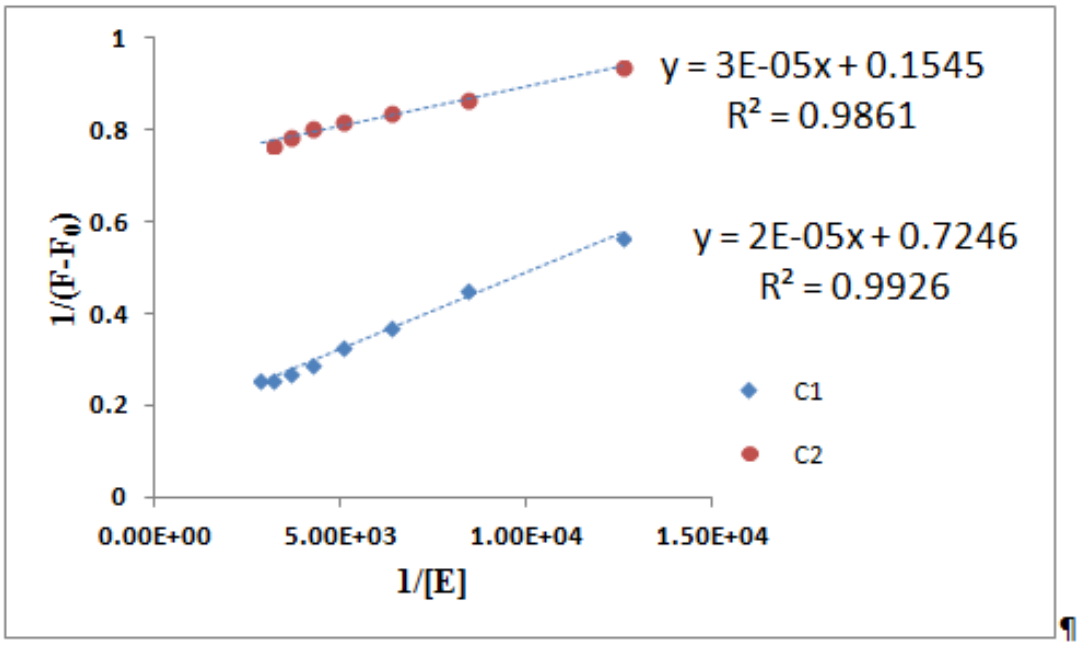

Figure6. The Lineweaver-Burk (LWB) plots (λ=526 nm) for (a) $\mathbf{C_1}$, (b) $\mathbf{C_2}$ at room temperature.

3.3.1. Effect of ionic strength on the complex-DNA binding

The phosphate backbone of DNA makes it an anionic polyelectrolyte, thus the change in ionic strength of medium is helpful for deducing the mode of binding. NaCl is a common salt for control the ionic strength of the solutions [56]. Generally, an electrostatic interaction occurs between cationic species (Na^+) and the negatively charged phosphate backbone of DNA. This interaction competes with the surface-binding of complexes and DNA. By following the spectral changes of complex-DNA after increasing the NaCl concentration, the mode of binding can be confirmed. In this study, however, no significant change connected with increasing the NaCl concentration occurred, suggesting that the mode of interaction between the complexes and DNA was not outside binding or electrostatic interaction Fig. 7(a).

3.3.2. Iodide quenching studies

ACCEPTED MANUSCRIPT

Using well-known quenchers like halide ions provides further evidence of the binding mode. Molecules which interact with DNA through the groove binding and particularly out site binding are accessible to the quencher, on the other hand, intercalators are protected by DNA pairs from being quenched [46,56-58]. Here, the iodide quenching experiment, the emission intensity of complexes-DNA solution in the absence and presence of potassium iodide remained unchanged. These results confirmed that the interaction of complexes with DNA was intercalation. Fluorescence plots of Iodide Quenching for $\mathbf{C_1}$ complex are shown in Fig. 7(b)

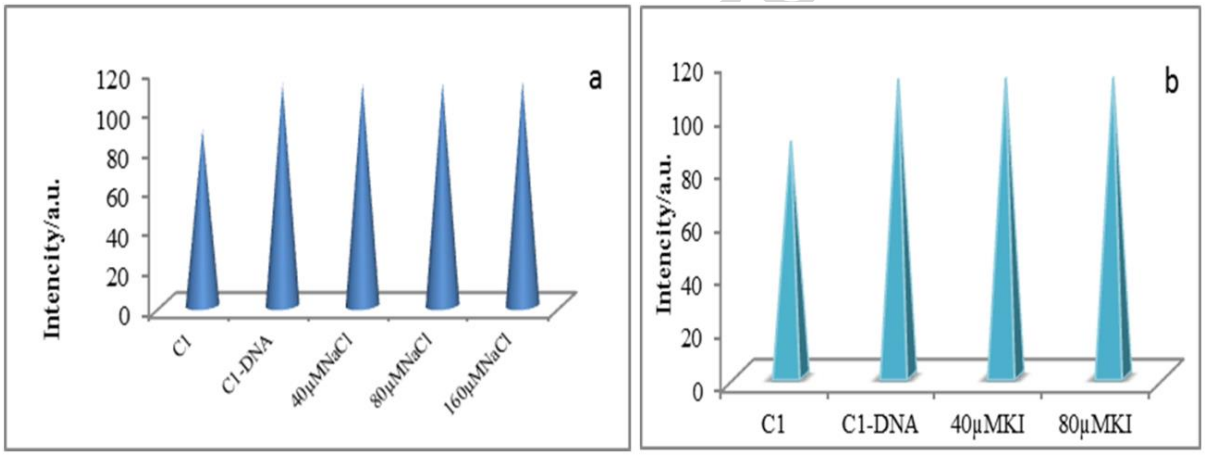

Figure7. Fluorescence plots of ionic strength (a) and Iodide Quenching (b) for $\mathbf{C_1}$ complex at room temperature.

3.4. Viscosity measurement

To further investigate the mode of binding between the complexes and DNA, viscosity measurement was carried out. Spectroscopic methods provide necessary evidence of the binding mode but sometimes they are not sufficient [4,57]. Hydrodynamic measurements which are sensitive to the change in DNA length are used to confirm the spectral data. Viscosity measurements determine unequivocally the binding mode in solution [4]. A classical intercalator increases the viscosity of DNA, due to increasing in the separation of the base pairs at the intercalation sites and consequently increasing the overall DNA length [59,60]. The values of

ACCEPTED MANUSCRIPT

(η/η_0) were plotted against [complex]/[DNA] for both complexes as shown in Fig. 8. The relative viscosity of DNA increased with increasing **C_1** and **C_2** concentration, indicating the classical intercalation mode of binding for both complexes. The viscosity of DNA was growing more by increasing **C_1** concentration showing that **C_1** intercalated more strongly and deeply than **C_2**. However increasing in viscosity for both complexes was lower than for ethidium bromide as a classical intercalator [50], Because of the nonplanar structure. The better intercalation of **C_1** compared with **C_2** can be explained by the more folded ligand structure.

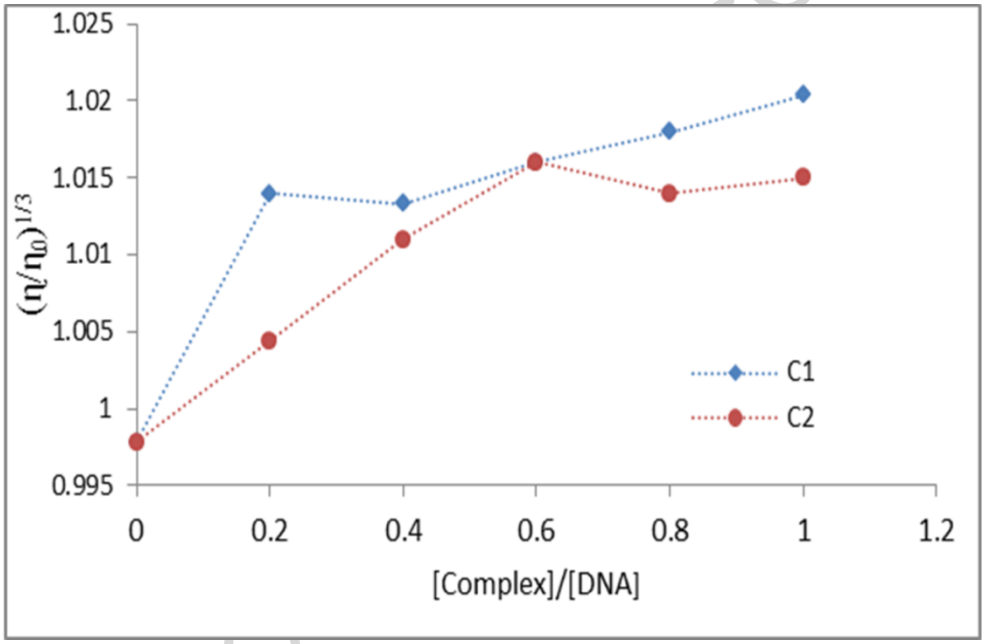

Figure8. Effect of increasing amounts of **C_1** and **C_2** on the viscosity of HS-DNA (100 µM) in 1mM tris-HCl buffer (r = 0.0-1) at 25°C

3.5. Molecular docking

Using the molecular docking technique is important in predicting the mode and affinity of drug-DNA interactions. This technique is useful to design molecules that can recognize specific sequences of DNA, as well as in the mechanistic studies and consists in placing a small molecule into the binding site of the specific target region of the DNA mainly in a noncovalent fashion

ACCEPTED MANUSCRIPT

[61]. Molecular docking studies of the two complexes with DNA were carried out in order to preliminarily predict the DNA-binding affinity as well as the preferred orientation of the docking pose. The lower Rerank Scores predicted the more binding affinity of the complexes to DNA. The negative values of Rerank Scores (Table 3) of the docked complexes indicated that the binding of the two complexes to the DNA is spontaneous. Therefore, on the basis of Rerank Scores results, the DNA binding affinity of complex **C_1** was stronger than that of complex **C_2**. (for **C_1**: -98.896 and for **C_2**: -83.213). Moreover, as shown in Fig. 9, the energy minimized docked poses obtained for both complexes suggested that two complexes were located in the minor grooves of DNA. This may occur due to the steric clashes between the complexes and DNA strand which inhibited the classical intercalation, and **C_1** with more folded ligand could insert deeper than **C_2**. Moreover, the orientation of the two complexes in the minor groove of DNA is different: **C_1** inserted from the coordinated nitrate groups which can interact through hydrogen binding to the DNA interior, but **C_2** inserted from an aromatic part of ligand. **C_2** with a less folded ligand cannot insert so deeply as **C_1**, in this case, only a part of the molecule comes between the two base pairs of DNA helix and makes stacking interactions between the ring system of the DNA bases and the phenyl ring of the complex. It is worthy to note that the binding of **C_1** with two additional OH groups on the ligand (one of them is coordinated to La and the other one is free) is stabilized by hydrogen binding. All these observations confirmed stronger binding affinity of **C_1**. Moreover attraction between positive charge of lanthanum and the negative phosphate backbones of DNA makes favorable the binding of the two complexes through electrostatic potentials.

ACCEPTED MANUSCRIPT

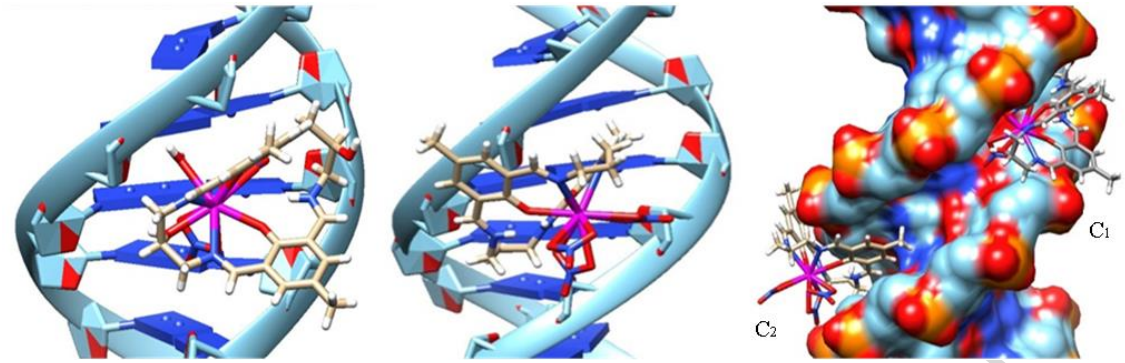

a b c

Figure9. Computational docking models (using the UCSF Chimera software) illustrating the mode of interaction between DNA and complexes (a) model of docking of **C_1**, b) **C_2** c) comparing the mode of binding of **C_1** and **C_2**.

Table 3. The values of Rerank Scores for C_1 and C_2 complexes obtained by docking studies

poses	**Rerank Scores (C_1)**	**Rerank Scores (C_2)**
1	**-98.896**	**-83.2131**
2	-88.5622	-80.7943
3	-82.5921	-80.5409
4	-78.179	-79.6746
5	-76.3901	-78.9394
6	-72.838	-78.7842
7	-72.3274	-78.7651
8	-71.7315	-78.7282
9	-69.8091	-77.6537
10	-68.8869	-77.5206

3.6. Cell viability:

Both tested complexes have no significant cytotoxic effect on Jurkat or MCF7 cell lines. The cell membrane is a semi-permeable barrier and although hydrophobic compounds move into the cell simply by diffusion, hydrophilic ones need specific transporters, channels or receptors to

ACCEPTED MANUSCRIPT

pass through the cells. The synthesized compounds have hydrophilic characters and probably would need suitable receptors for entering the cells. The missing cytotoxic effect of the compounds might be due to the lack of ability to path through the cell membrane, or due to the participation of the compounds in irreversible interactions with the fetal bovine serum albumin or other proteins in the culture medium.

3.7. Circular Dichroism (CD) studies

CD spectroscopy is a useful technique in diagnosing changes in DNA structure during drug-DNA interactions. The CD spectrum of FS-DNA exhibits a positive band at 275 nm due to the base stacking and a negative band at 248 nm due to the right-handed helicity of B-DNA form which is quite sensitive to the mode of DNA interactions with small molecules [62,63]. Simple groove binding and electrostatic interaction of small molecules with DNA shows less or no perturbation on the base stacking and helicity bands while intercalators enhance the intensities of both the bands, stabilizing the right-handed B conformation of DNA [61]. The CD spectrum of FS-DNA in the absence and presence of the complexes are shown in Fig. 10. The measurement confirmed the intercalation mode of binding of the complexes with DNA.

ACCEPTED MANUSCRIPT

ACCEPTED MANUSCRIPT

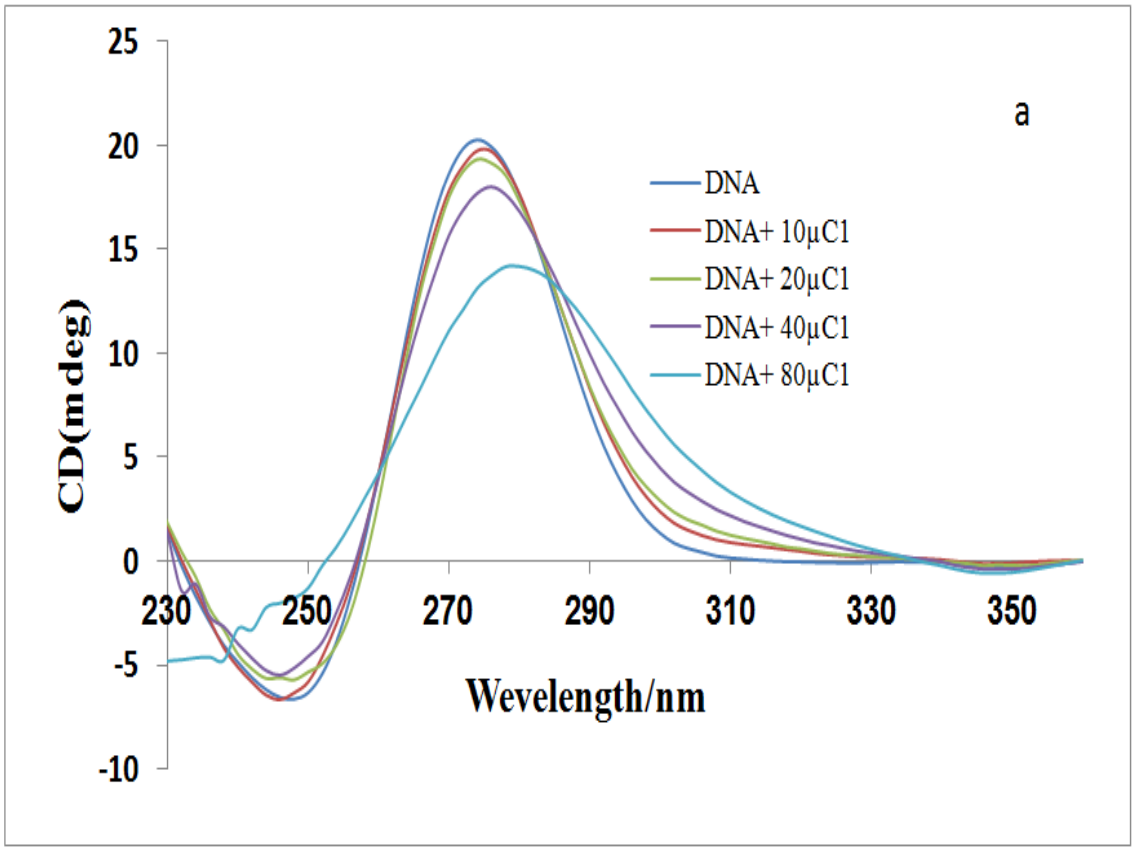

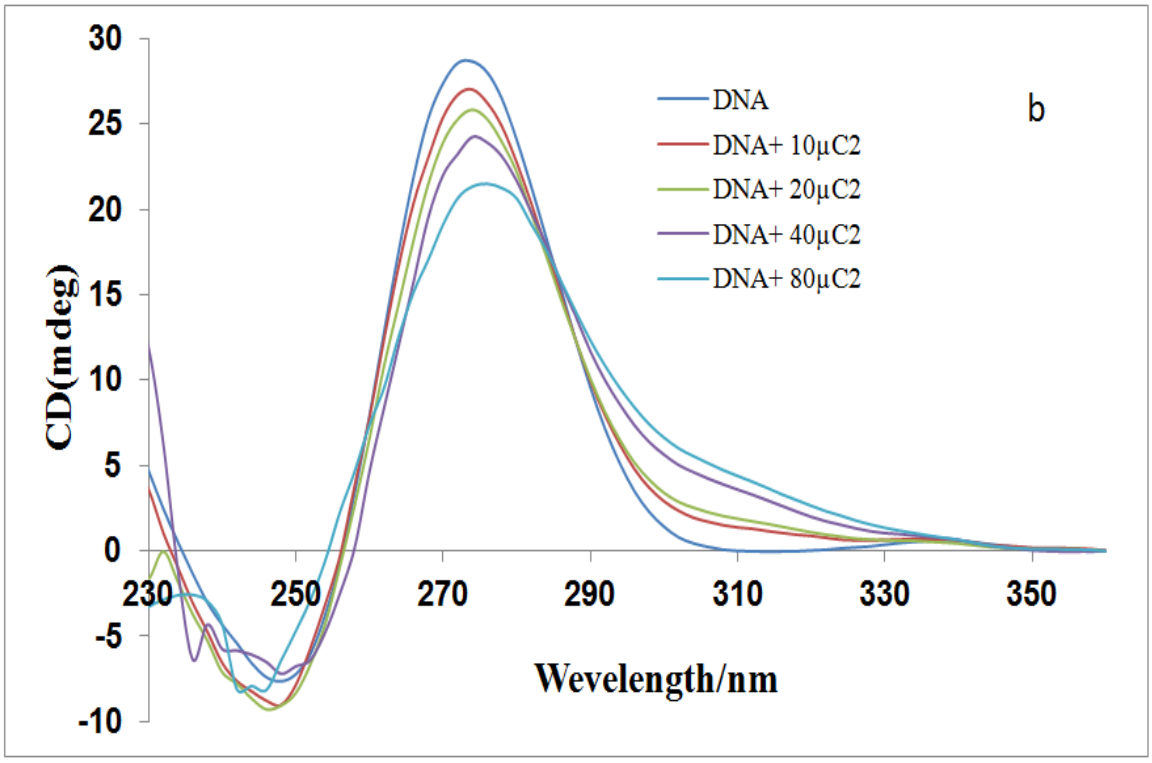

ACCEPTED MANUSCRIPT

Figure10. Effect of $\mathbf{C_1}$ **&** $\mathbf{C_2}$ on CD spectrum of FS-DNA (200 μM) with varying concentration of $\mathbf{C_1}$ (a) and $\mathbf{C_2}$ (b) at 25°C

3.8. Results of DNA cleavage study

The chemical nuclease activities of the complexes have been studied using supercoiled pBluescript plasmid DNA in phosphate buffer saline (PBS), pH □ 7.4 in the absence of a reducing agent under physiological conditions. A classical intercalator: ethidium bromide was used for comparison. As shown in Fig. 11, in the case of $\mathbf{C_1}$, SC DNA faded along with increasing of the complex concentration (line 1, 2, and 3). Based on gel electrophoresis data, the $\mathbf{C_1}$ it might replaces the ethidium bromide in DNA structure in a competitive manner and in the presence of increasing concentration of $\mathbf{C_1}$ from 50 to 200 μM, ethidium bromide could not bind to DNA. It was understood from DNA viscosity measurement that ethidium bromide increases DNA length more than $\mathbf{C_1}$. However, the positive charge of lanthanum in $\mathbf{C_1}$ along with using in high concentration in compare to ethidium bromide (1mg/ml) may cause the ethidium bromide substitution in the DNA electrophoresis assay. Compound $\mathbf{C_2}$ had no nuclease effect on SC DNA (line 4, 5 and 6) and although based on UV spectroscopic study, $\mathbf{C_2}$ can bind to DNA with binding constant of 5.2×10^3; it was not shown any changes in electrophoretic mobility of the circular DNA.

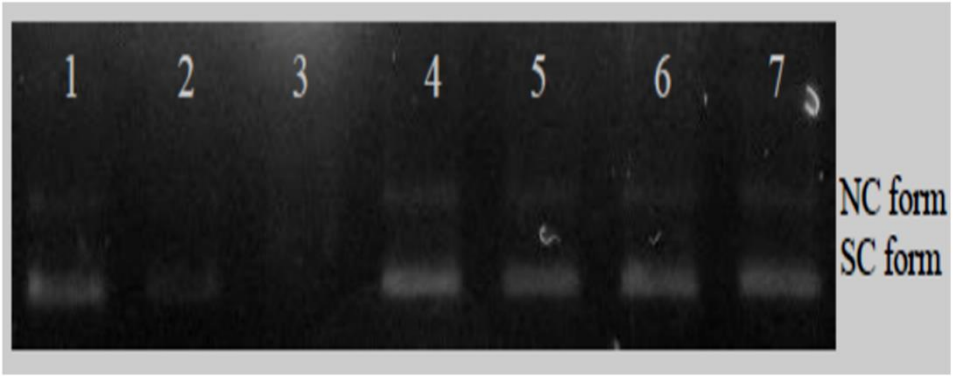

ACCEPTED MANUSCRIPT

Figure11. Gel electrophoresis of plasmid DNA treated with the complexes $\mathbf{C_1}$ and $\mathbf{C_2}$ in dark. Lane 1, 2, and 3 indicated DNA treated with $\mathbf{C_1}$ at 50, 100, and 200 μM concentrations, respectively. Lane 4, 5, 6 represent DNA treated with $\mathbf{C_2}$ at 50, 100, and 200 μM concentrations, respectively. Lane 7 indicates control (no compound treatment.)

3.9. Cell toxicity

Both tested complexes had no significant cytotoxic effect on Jurkat and MCF7 cancerous cell lines in their free forms. These data revealed that the cell membrane is probably a problem for the compounds effect especially for $\mathbf{C_1}$ which has more hydrophilic nature. The cell membrane is a semi-permeable barrier and although hydrophobic compounds move into the cell simply by diffusion, hydrophilic ones need specific transporters, channels or receptors to pass through cells. The synthesized compounds have hydrophilic characters and probably need suitable receptors for entering to the cells. So having no cytotoxicity effect of the compounds might be due to the lack of ability to pass through the cell membrane, or due to the participation of the compounds in irreversible interactions with fetal bovine serum albumin or other proteins in a culture medium which leads to not free to inter the cells. To evaluate this hypothesis, chitosan coated MNPs was used as a carrier for loading of the compounds. Cell cytotoxicity assay for both loaded complexes was conducted in a variety of concentrations from 50 to 300 μg/ml in a 48 hours period of time. The result was surprising and the IC_{50} value for $\mathbf{C_1}$ loaded CS-MNPs was estimated 245.1 ± 5.2 μg/ml on HepG2 hepatoma cell line. Nevertheless, $\mathbf{C_2}$ loaded CS-MNPs had no significant cytotoxicity effect up to 300 μg/ml. These results point out that CS-MNPs possess apparent target ability to the surface of glucose overexpressed cells (cancerous cell lines) and can efficiently deliver and release the complexes into target cancer cells. But based on the $\mathbf{C_1}$ and $\mathbf{C_2}$ loading efficiency and their effect on DNA, the result was different. Since the $\mathbf{C_1}$ and $\mathbf{C_2}$ encapsulation

ACCEPTED MANUSCRIPT

capacity on CS-MNPs are 29% and 14.2%m respectively and the **C_1** was more effect on DNA structure, the present data are plausible.

4. Conclusions:

Two water-soluble macrocyclic Schiff base lanthanum (III) complexes were synthesized and characterized. X-ray crystallographic data for **C_1** revealed a mononuclear ten-coordinated complex. The binding property of the complexes with Fish DNA under physiological conditions has been studied using UV-Vis spectrophotometry, DNA viscosity measurements, circular dichroism (CD), fluorescence spectroscopy, agarose gel electrophoresis and molecular docking. The results showed that the main binding mode of the complexes to DNA was intercalation. It is likely to have hydrogen bonding and electrostatic attraction between the complexes and DNA in the binding mode, as well. Structural differences of the complexes were important in binding affinity of the compounds. Moreover, the DNA docking studies suggested that the complexes interacted in the minor groove of DNA. The docking results also revealed the higher binding affinity of **C_1** compared to **C_2**. Based on the gel electrophoresis study, the **C_1** was more effective than **C_2** on DNA structure and SC DNA faded along with increasing its concentration up to 200 μM. Moreover, this result suggests that the **C_1** complex can compete for DNA-binding sites of ethidium bromide which is usually characteristic of potent DNA intercalators. The cytotoxicity data showed that polarity of compounds is also an important factor in anticancer drugs design and must be considered in their synthesis.

The results of this study revealed that the structural feature of complexes can influence on the DNA binding affinity which is useful in the design of the new metal-base drugs.

ACCEPTED MANUSCRIPT

Acknowledgements

We are grateful to the Shiraz university research council for its financial support. The crystallographic part was supported by the project 15-12653S of the Czech Science Foundation using instruments of the ASTRA lab established within the Operation program Prague Competitiveness - project CZ.2.16/3.1.00/24510.

ACCEPTED MANUSCRIPT

ACCEPTED MANUSCRIPT

References:

[1] B.-d. Wang, Z.-Y. Yang, T.-r. Li, Bioorg. Med. Chem. 14 (2006) 6012-6021.

[2] E. Meggers, Curr. Opin. Chem. Biol. 11 (2007) 287-292.

[3] A. Lauria, R. Bonsignore, A. Terenzi, A. Spinello, F. Giannici, A. Longo, A.M. Almerico, G. Barone, Dalton Trans. 43 (2014) 6108-6119.

[4] S.S. Bhat, A.A. Kumbhar, H. Heptullah, A.A. Khan, V.V. Gobre, S.P. Gejji, V.G. Puranik, Inorg. Chem. 50 (2010) 545-558.

[5] V. Rajendiran, R. Karthik, M. Palaniandavar, H. Stoeckli-Evans, V.S. Periasamy, M.A. Akbarsha, B.S. Srinag, H. Krishnamurthy, Inorg. Chem. 46 (2007) 8208-8221.

[6] A. Arbuse, M. Font, M.A. Martínez, X. Fontrodona, M.J. Prieto, V. Moreno, X. Sala, A. Llobet, Inorg. Chem. 48 (2009) 11098-11107.

[7] P. Kumar, S. Gorai, M.K. Santra, B. Mondal, D. Manna, Dalton Trans. 41 (2012) 7573-7581.

[8] C. Rajarajeswari, R. Loganathan, M. Palaniandavar, E. Suresh, A. Riyasdeen, M.A. Akbarsha, Dalton Trans 42 (2013) 8347-8363.

[9] K. Wu, S. Liu, Q. Luo, W. Hu, X. Li, F. Wang, R. Zheng, J. Cui, P.J. Sadler, J. Xiang, Inorg. Chem. 52 (2013) 11332-11342.

[10] H. You, H. Spaeth, V. Linhard, A. Steckl, Langmuir 25 (2009) 11698-11702.

[11] X. Pei, J. Zhang, J. Liu, J. Mol. Clin. Oncol. 2 (2014) 341-348.

[12] K.D. Mjos, C. Orvig, Chem. Rev. 114 (2014) 4540-4563.

[13] M. Sirajuddin, S. Ali, A. Badshah, J. photochem. Photobio. B 124 (2013) 1-19.

[14] C. Silvestri, J.S. Brodbelt, Mass Spectrom. Rev. 32 (2013) 247-266.

ACCEPTED MANUSCRIPT

[15] Z. Ma, J.R. Choudhury, M.W. Wright, C.S. Day, G. Saluta, G.L. Kucera, U. Bierbach, J. Med. Chem. 51 (2008) 7574-7580.

[16] C. Icsel, V.T. Yilmaz, DNA Cell Biol. 32 (2013) 165-172.

[17] Q. Wang, Z.-Y. Yang, G.-F. Qi, D.-D. Qin, Eur. J. Med. Chem. 44 (2009) 2425-2433.

[18] H. Wu, G. Pan, Y. Bai, Y. Zhang, H. Wang, F. Shi, X. Wang, J. Kong, J. photochem. Photobio. B 135 (2014) 33-43.

[19] A. Krężel, J. Lisowski, J. Inorg. Biochem. 107 (2012) 1-5.

[20] Y.-C. Liu, Z.-F. Chen, X.-Y. Song, Y. Peng, Q.-P. Qin, H. Liang, Eur. J. Med. Chem. 59 (2013) 168-175.

[21] D. Parker, R.S. Dickins, H. Puschmann, C. Crossland, J.A. Howard, Chem. Rev. 102 (2002) 1977-2010.

[22] S. Kariminia, A. Shamsipur, M. Shamsipur, J. Pharm. Biomed. Anal. 129 (2016) 450-457.

[23] Y. Ding, S.Z. Shen, H. Sun, K. Sun, F. Liu, Y. Qi, J. Yan, Mater. Sci. Eng. C Mater. Biol. Appl. 48 (2015) 487-498.

[24] G. Prabha, V. Raj, J. Magn. Magn. Mater. 408 (2016) 26-34.

[25] M. Parsian, G. Unsoy, P. Mutlu, S. Yalcin, A. Tezcaner, U. Gunduz, Eur. J. Pharmacol. 784 (2016) 121-128.

[26] C.N. Verani, E. Rentschler, T. Weyhermüller, E. Bill, P. Chaudhuri, J. Chem. Soc., dalton trans. (2000) 251-258.

[27] P. Bag, S. Dutta, U. Flörke, K. Nag, J. Mol struct. 891 (2008) 408-419.

[28] D.C. Cupertino, R.W. Keyte, A.M. Slawin, J.D. Woollins, Polyhedron 18 (1998) 311-319.

[29] L. Palatinus, G. Chapuis, J. Appl crystallogr. 40 (2007) 786-790.

[30] V. Petříček, M. Dušek, L. Palatinus, Z. Kristallogr. 229 (2014) 345-352.

ACCEPTED MANUSCRIPT

[31] G.-J. Chen, Z.-G. Wang, X. Qiao, J.-Y. Xu, J.-L. Tian, S.-P. Yan, J. Inorg. Biochem**.** 127 (2013) 39-45.

[32] L. Cabeza, R. Ortiz Quesada, J.L. Arias Mediano, A. Ruiz Martínez, J.M. Entrena Fernández, R. Luque Caro, C. Melguizo Alonso, (2015).

[33] M.G. Pineda, S. Torres, L.V. López, F.J. Enríquez-Medrano, R.D. De León, S. Fernández, H. Saade, R.G. López, Molecules 19 (2014) 9273-9287.

[34] R. Thomsen, M.H. Christensen, J. Med. Chem. 49 (2006) 3315-3321.

[35] M.A. Lie, R. Thomsen, C.N. Pedersen, B. Schiøtt, M.H. Christensen, J. Chem. Inf. Model. 51 (2011) 909-917.

[36] F. Keshavarz, D. Mohammad-Aghaie, Phys. Chem. Res. 3 (2015) 125-143.

[37] P. Bag, U. Flörke, K. Nag, Dalton Trans. (2006) 3236-3248.

[38] A. Pui, T. Malutan, L. Tataru, C. Malutan, D. Humelnicu, G. Carja, Polyhedron 30 (2011) 2127-2131.

[39] G.-J. Chen, X. Qiao, C.-Y. Gao, G.-J. Xu, Z.-L. Wang, J.-L. Tian, J.-Y. Xu, W. Gu, X. Liu, S.-P. Yan, J. Inorg. Biochem**.** 109 (2012). 90-96.

[40] X.-W. Liu, Y.-M. Shen, Z.-X. Li, X. Zhong, Y.-D. Chen, S.-B. Zhang, Spectrochim. Acta A Mol. Biomol. Spectrosc. 149 (2015) 150-156.

[41] X.-L. Li, Y.-J. Hu, H. Wang, B.-Q. Yu, H.-L. Yue, Biomacromolecules 13 (2012) 873-880.

[42] J. Liu, H. Zhang, C. Chen, H. Deng, T. Lu, L. Ji, Dalton Trans. (2003) 114-119.

[43] G. Barone, A. Terenzi, A. Lauria, A.M. Almerico, J.M. Leal, N. Busto, B. García, Coordin. Chem. Rev. 257 (2013) 2848-2862.

[44] N. Shahabadi, S. Kashanian, F. Darabi, Eur. J. Med. Chem. 45 (2010) 4239-4245.

[45] M.T. Carter, M. Rodriguez, A.J. Bard, J. Am. Chem. Soc. 111 (1989) 8901-8911.

ACCEPTED MANUSCRIPT

[46] Z.-u. Rehman, A. Shah, N. Muhammad, S. Ali, R. Qureshi, A. Meetsma, I.S. Butler, Eur. J. Med. Chem. 44 (2009) 3986-3993.

[47] M.A. Ragheb, M.A. Eldesouki, M.S. Mohamed, Spectrochim. Acta A Mol. Biomol. Spectrosc. 138 (2015) 585-595.

[48] R. Eswaran, R. Bertani, P. Sgarbossa, N. Karuppannan, J. Inorg. Biochem**.** 155 (2016) 1-8.

[49] M.F. Hassan, A. Rauf, Spectrochim. Acta A Mol. Biomol. Spectrosc. 153 (2016) 510-516.

[50] B.-d. Wang, Z.-Y. Yang, M.-h. Lü, J. Hai, Q. Wang, Z.-N. Chen, J. Organomet. Chem. 694 (2009) 4069-4075.

[51] F. Arjmand, A. Jamsheera, Spectrochim. Acta A Mol. Biomol. Spectrosc. 78 (2011) 45-51.

[52] N. Shahabadi, S. Kashanian, F. Darabi, DNA Cell Biol. 28 (2009) 589-596.

[53] F. Samari, B. Hemmateenejad, M. Shamsipur, M. Rashidi, H. Samouei, Inorg. Chem. 51 (2012) 3454-3464.

[54] A. Moodi, M. Khorasani-Motlagh, M. Noroozifar, S. Niroomand, J. Biomol. Struct. Dyn. 31 (2013) 937-950.

[55] M. Anjomshoa, H. Hadadzadeh, M. Torkzadeh-Mahani, S.J. Fatemi, M. Adeli-Sardou, H.A. Rudbari, V.M. Nardo, Eur. J. Med. Chem. 96 (2015) 66-82.

[56] M. Khorasani-Motlagh, M. Noroozifar, A. Moodi, S. Niroomand, J. photochem. Photobio. B. 127 (2013) 192-201.

[57] G. Zhang, X. Hu, N. Zhao, W. Li, L. He, Pestic. Biochem. Phys. 98 (2010) 206-212.

[58] F. Jalali, G. Rasaee, Int. J. Biol. Macromol. 81 (2015) 427-434.

[59] A. Manna, S. Chakravorti, Spectrochim. Acta A Mol. Biomol. Spectrosc. 150(2015) 120-126.

[60] S. Ramakrishnan, M. Palaniandavar, Dalton Trans. (2008) 3866-3878.

ACCEPTED MANUSCRIPT

[61] K. Zheng, L. Zhu, Y.-T. Li, Z.-Y. Wu, C.-W. Yan, J. Photochem. Photobiol. B, Biol. 149 (2015) 129-142.

[62] A. Bonincontro, M. Falivene, C. La Mesa, G. Risuleo, M. Ruiz Peña, Langmuir 24 (2008). 1973-1978.

[63] T. Sarwar, S.U. Rehman, M.A. Husain, H.M. Ishqi, M. Tabish, Int. J. Biol. Macromol. 73 (2015) 9-16.

ACCEPTED MANUSCRIPT

ACCEPTED MANUSCRIPT

Graphical Abstract

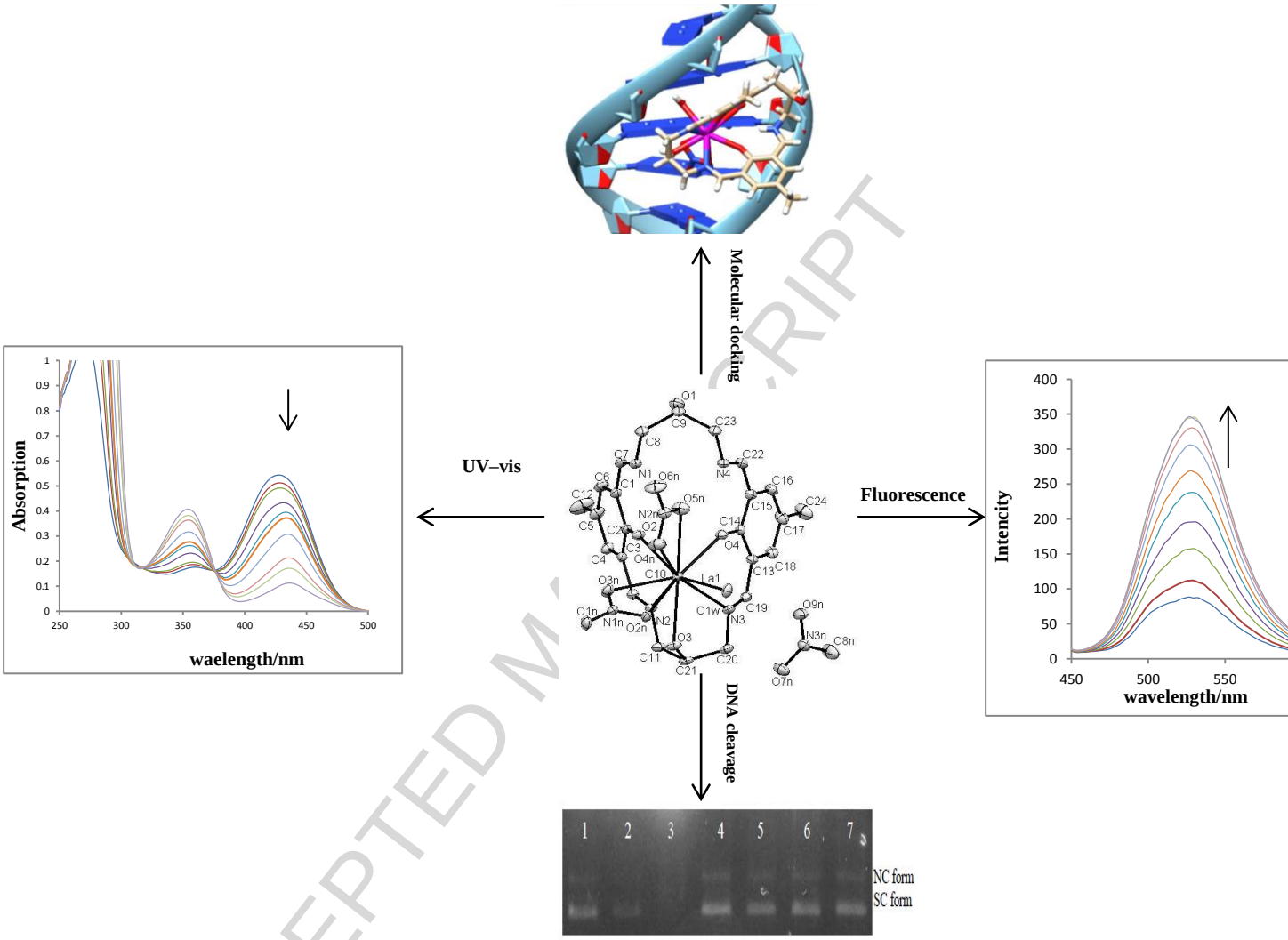

ACCEPTED MANUSCRIPT

Highlights

- Water-soluble mono-nuclear macrocyclic lanthanum(III) complexes were synthesized and characterized.
- The interaction of complexes with DNA was studied.
- Docking studies was done to confirm the mode of binding.
- Cytotoxic activity of chitosan-coated magnetic nanoparticles as drug delivery for the complexes was studied.

ACCEPTED MANUSCRIPT